Surface & Coatings Technology 205 (2011) 5478–5482

Contents lists available at ScienceDirect

Surface & Coatings Technology

journal homepage: www.elsevier.com/locate/surfcoat

Application of acoustic emission to detect damage mechanisms of particulate filled thermoset polymeric coatings in four point bend tests

Y. Xu *, B.G. Mellor

Materials Research Group, School of Engineering Sciences, University of Southampton, Highfield, Southampton, SO17 1BJ, UK

ARTICLE INFO

Article history:
Received 23 October 2010
Accepted in revised form 10 June 2011
Available online 25 June 2011

Keywords:
Acoustic emission
Filled polymeric coatings
Four point bend test
Failure modes

ABSTRACT

In this study, particulate filled thermoset polymeric coatings with two different coating thicknesses were subjected to four point bend loading while being monitored by acoustic emission in order to establish the failure modes of the filled polymeric coatings. The polymeric coatings were approximately 260 μm and 350 μm in thickness on a steel substrate, and filled with 9% by volume of calcium silicate. After testing the thinner coating was found to exhibit more microcracks on the surface of the coating while the thicker coating showed more extensive delamination between the coating layer and the steel substrate. A noticeable load relaxation was observed during the plastic deformation of the coating samples which was coincident with an increase in acoustic emission. This was linked to the development of macrocracks and their propagation through the coating thickness. The number and amplitude of the acoustic emission events were investigated and correlated with the failure mechanisms present during the four point bend test, such as debonding of the embedded fillers, delamination of the coating layer from the substrate and the initiation and propagation of cracks. This then allows the failure modes of particulate filled thermoset coatings and their location to be identified from the acoustic emission detected during the four point bend test.

1. Introduction

Composite materials generally exhibit a variety of failure modes including matrix cracking, debonding, fibre breakage resulting from the statistical distribution of fibre strength, delamination, and void growth [1]. Acoustic emission (AE) can be defined as transient elastic stress waves, generated at a source by the rapid release of strain energy within a material [2]. The technique of acoustic emission is thus ideally suited to study stress dependent damage processes in fibre composites as it permits real-time monitoring of damage processes as a function of changes in time and load level, has high sensitivity (e.g. individual filament fractures, individual filament debonding, as well as matrix cracking and delamination can all be monitored) and allows the location of regions in the sample at which damage is accumulating, etc. [3]. In addition, the technique of AE has been widely applied to four point bend tests and used in evaluating the properties of thermal sprayed coatings [4–6]. Crack initiation and propagation in these coatings can be inferred from analysis of the AE signals detected in terms of their absolute energy, amplitude and number of hits [7–14]. However, although AE technology has been extensively applied to the study of failure mechanisms in polymeric composite materials [15–18] and metallic coatings [19,20] few studies have been dedicated to polymeric coatings [21,22] and no reports of AE of particulate filled polymeric coating materials were found in a literature survey conducted using ISI Web of Knowledge[SM].

Thus in the present study, four point bend tests were carried out on particulate filled polymeric coated samples, the acoustic emission technique being employed to examine in-situ cracking during the four point bend tests. The different failure modes of the coating material were correlated with the loading conditions and AE signals obtained during the test process.

2. Experimental

2.1. Characterisation of particulate filled thermoset polymeric coatings

Two types of thermoset polymeric coating, designated as T-15A and T-15B, manufactured by the method of thermal spray on mild steel substrate were used in this study. T-15A and T-15B are modified novolac thermoset polymeric coatings; the major difference between them is the coating thickness, T-15A approximately 260 μm, T-15B 350 μm. Fig. 1 represents a transverse section of the T-15A coating, the fillers ($CaSiO_3$), which constitute approximately 9% by volume in this coating, are well bonded with the coating matrix. Detailed information of the coatings T-15A and T-15B are listed in Table 1.

The polymeric coating samples were cut into test pieces 90 mm in length and 18 mm in width in order to be of a suitable size for the four point bend test rig and the AE sensors used. The steel substrates of all the test coatings were machined to 1.5 mm thick. Therefore, the

* Corresponding author at: School of Engineering and Design, Brunel University, Uxbridge UB8 3PH, UK. Tel.: +44 1895 265883; fax: +44 1895 269861.
E-mail address: yanmeng.xu@brunel.ac.uk (Y. Xu).

0257-8972/$ – see front matter © 2011 Elsevier B.V. All rights reserved.
doi:10.1016/j.surfcoat.2011.06.021

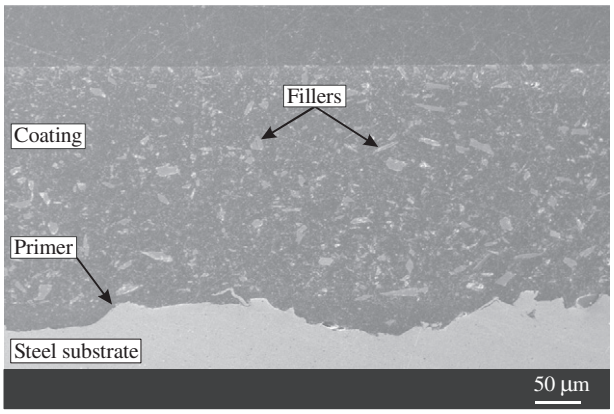

Fig. 1. SEM image of a transverse section of the T-15B coating. Note the two shapes (angular and flake) of filler particles.

influence of the steel substrate thickness on the behaviour of the different polymeric coatings was negligible.

2.2. Experimental process

Four point bend tests were carried out on an Instron 8874 Servohydraulic testing machine. A four point bend test attachment including an aluminium block with two grooves and four ceramic rollers was used to support the specimen and the load cell. The coating was loaded so that it was subjected to tensile stresses. Two ceramic rollers were fitted in the grooves on the aluminium block to support the test specimen and the other two rollers were put on the surface of the steel substrate of the sample to support the load applied from the Instron machine. The inner span length (distance between centres of the two rollers on the steel substrate) was 20 mm and the outer span length (distance between centres of the two rollers supporting the specimen) was 40 mm.

In the present study, Vallen AE-Suite equipment was used to monitor the in-situ cracking of the specimen during the four point bend tests. One PZT transducer was mounted on each end of the samples to detect the presence of the AE signals generated. As both transducers detect signals originating from the same source, a time lag exists between the detection of the event by each of the two transducers depending on the location of the signal source. The difference between the times of first count over the predefined threshold is used to calculate the location of the signal source. The AE system also consists of a signal processor unit (SPU). Different thresholds can be set in the SPU for different specimens in order to filter unwanted AE signals. While the test was being carried out, the signals obtained could be displayed on a monitor. With this AE system, the locations of the AE events in the test sample are calculated corresponding to the positions (Channel Positions) of the two PZT transducers which are entered into the SPU before starting each experiment. The "Channel Positions" were determined by the following procedure: the centre of the first transducer (channel) is set as the zero point and the distance between the centres of the two transducers is set as the position of the second channel. This assumes that the AE signals are collected at the centres of the transducers. The value of "Channel Positions" is important, so that the location of the events can be determined by the AE system. The relative positions of the PZT transducers and supporting rollers are schematically described in Fig. 2 based on the size of test specimens and test rig.

The load was applied at a constant crosshead speed of 0.3 mm/min, the distance that the crosshead (load cell of the Instron machine) moved was fixed at 4 mm for all the specimens tested.

The threshold parameter in the tests was set at 52 dB to avoid unwanted AE events, which were possibly generated by background noise or friction between the steel substrate and the ceramic rollers. The threshold set was based on a large number of experiments on uncoated mild steel specimens under the same experimental conditions as for the polymeric coatings.

In all of the previous trial tests, including the test results discussed in this paper, no damage in the form of cracks or severe plastic deformation was noted to occur on the two thermoset coating surfaces in contact with the rollers. The above experimental set up was therefore suitable to collect AE data which was not influenced by the direct contact of the coating and the ceramic rollers. This will be further demonstrated by the experimental results discussed below.

2.3. Experimental results and discussion

Fig. 3 shows the top view (a), and the side view (b), of the thermoset coating samples T-15A and T-15B after testing. Two macrocracks are visible on the surface of coating T-15B, while two macrocracks with three microcracks are evident on the surface of the coating T-15A. The thicker coating T-15B exhibits more extensive delamination between the coating layer and the steel substrate than the thinner coating T-15A.

Fig. 4(a) and (b) shows the traces revealing the relationship between the number of AE events, load and the deformation of the coating samples T-15A and T-15B. From the upper limit of the linear slope of the load–displacement curves in (a) and (b), the yield load of the two coating specimens was determined to be similar at 0.65 kN. Note the yield load of the two samples are almost the same, although the two coatings have different thicknesses of 250–270 μm and 345–360 μm. This is because the coating has very low strength and stiffness compared to the substrate steel so the significant differences in thickness of the polymeric coating will not affect the yield load of the coated sample.

Table 1
Details of the modified Novolac coatings.

Designation	T-15A	T-15B
Colour	Dark green	Dark green
Polymer base	Thermoset	Thermoset
Resin type	Modified novolac (powder)	Modified novolac (powder)
Filler type	$CaSiO_3$	$CaSiO_3$
Filler percentage	9%	9%
Filler size (μm)	10–30	10–30
Filler shape	Angular and flake morphology	Angular and flake morphology
Matrix thickness (μm)	250–270	345–360
Primer type	Phenolic	Phenolic
Primer thickness (μm)	15–30	20–30

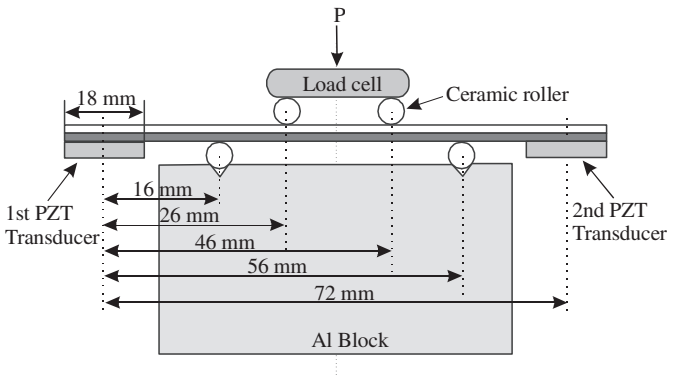

Fig. 2. Schematic diagram representing the detailed relative positions of the parts of the test system.

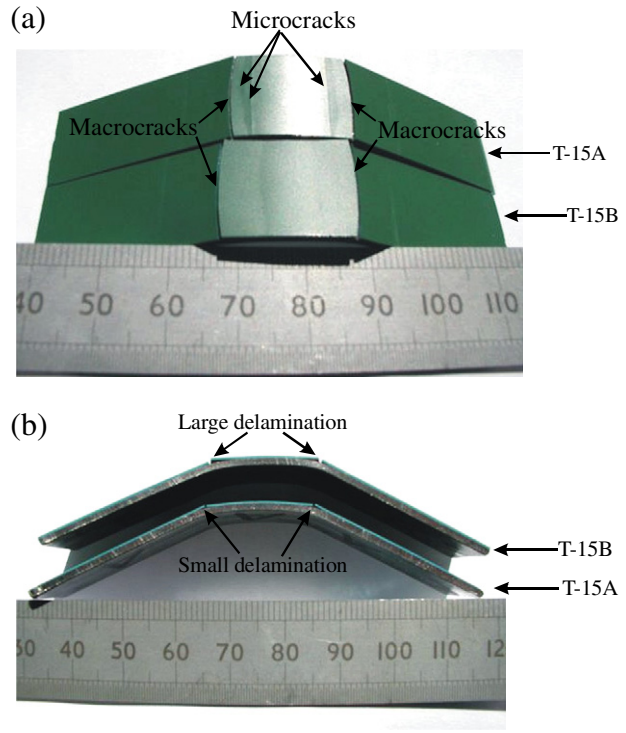

Fig. 3. Top and side views of the thermoset coatings T-15A and T-15B after testing. (a) Surface of coating specimens T-15A and T-15B showing two macrocracks on the surface of T-15B and two macrocracks with three microcracks on the surface of T-15A. (b) Side view of coating T-15A and T-15B showing differences in the size of the delaminations found in the two coatings after testing.

No AE events were observed until a compressive load of 0.93 kN was reached; after this, the number of AE events began to increase, simultaneously there was an apparent relaxation in the load (see Fig. 4(a) and (b)), which could possibly be associated with the cracking of the coating. When similar four point bend tests were carried out on steel samples coated with a ductile thermoplastic polymeric material which did not exhibit cracking no load drop was ever noted indicating that this load drop is indeed associated with cracking phenomenon and is not an experimental artefact. Cracking of the coating leads to an effective reduction in I (second moment of area) and for a given displacement this results in a lower load. Visual examinations of both test specimens shown in Fig. 3(a) and (b) help substantiate this conclusion. It is noted that the load drop occurred when the coating samples were behaving plastically with a much smaller apparent modulus than the normal elastic value of 207 GPa. The modulus of the particulate filled thermoset coating (<20 GPa) will under these conditions have a relatively larger effect on the overall stiffness of the test samples, i.e. a load drop might be expected to be observed when the macrocracks develop and propagate through the coating thickness. Nevertheless, if the cracks in the coating occurred when the steel substrate was still behaving elastically a load drop would not be expected to be large enough to be observed as the coating then has relatively little effect on the total stiffness of the sample. The numbers of cracks on the two specimens, especially the macrocracks, were coincident with the number of the relaxations of load on the load–displacement curves found in Fig. 4(a) and (b). This further suggests that the cracking of the coating surface produced the relaxation of load recorded.

Two differences are evident between coating specimens T-15A and T-15B with respect to their relaxations in load on the load–displacement curves during their plastic deformation. First, the amplitudes of the relaxations between the two types of coated specimens are obviously different. The amplitude of the first relaxation of the coating T-15B was approximately 0.09 kN (from 0.97 to 0.88 kN), and the second one is about 0.08 kN; whereas, the amplitudes of the first and second relaxations of the coating T-15A were only about 0.015 and 0.022 kN (from 0.92 to 0.9 kN). This was because the crack in the thinner coating leads to only a slight change in the overall second moment of area. In addition, if this macrocrack does not lead to extensive delamination the coating between the two inner rollers will still take some load and thus can crack again, leading to a further, albeit smaller, load drop. The evidence that coating T15-A exhibits smaller delaminations but with more microcracks on the coating surface than T15-B (Fig. 3) suggests that this is occurring. Second, the intervals between the first two relaxations of the load for the two coatings are different representing different times between the first two cracks. The interval for the T-15A was much shorter than that for the T-15B, this indicates that it took a longer time to produce another crack for the T-15B after the first one because the applied load decreased significantly so that a longer time was required for the load to reach the level which was high enough to produce the next crack.

Fig. 4(c) and (d) shows the AE amplitudes for the coating samples T-15A and T-15B. The AE signals can be approximately divided into four domains: few signals are found between 85 dB and 95 dB; a larger number of events occurred from 70 dB to 85 dB; an even greater number of events occurred between 60 dB and 70 dB; the largest number of events occurred between 52 dB and 60 dB. The amplitudes of all the AE events were beyond 52 dB, since the threshold in the AE system has been set to this level in order to filter out the AE signals resulting from the noise or friction. Note that for coating T-15A signals of amplitude 95 dB were collected from the beginning of AE emission (when the deflection of the test sample was 38.8 mm) until the end of the test, but for coating T-15B signals of this amplitude were only found between the beginning of AE emission (when the deflection of the test sample was 38.6 mm) until 39.5 mm deflection of the test sample. The cumulative energies of the AE signals detected during the tests are also shown in the figures: at the end of the test these values are approximately 18E4 eu and 21E4 eu for the two sensors in the test for T-15A, and 35E4 eu for the two sensors in the test for T-15B. The higher cumulative energy recorded for T15-B than T15-A is linked to the greater number of AE events collected for T-15B than for T15-A as shown in Fig. 4(a) and (b). The AE signals can be associated with four possible mechanisms: initiation of cracks; propagation of cracks; delaminations of the coating from the steel substrate; debonding or cracking of the embedded fillers in the coating.

Fig. 4(e) is the graph of the number of events with respect to their locations for coating sample T-15A; Fig. 4(f) gives the filtered data from Fig. 4(e) (filter condition: 70 dB≤Amplitude≤95 dB). It is apparent from Fig. 4(f) that most of the high amplitude events were located at positions where the two macrocracks and three microcracks occurred. This indicates that the amplitudes for the initiation and propagation of cracks fall into the 70 dB and 95 dB region. As it is known that the number of events caused by the initiation of the cracks should be less than that corresponding to the propagation of cracks it can therefore be concluded that the AE amplitude for the initiation of cracks is between 85 dB and 95 dB; and the amplitude for the propagation of cracks is less than that required for initiation and falls between 70 dB to 85 dB. Furthermore, many signals with amplitudes between 60 dB and 85 dB are found close to the positions of the cracks shown in (e). These are considered to be caused by delamination of the coating from the steel substrate. Consequently, the large number of remaining signals with amplitude between 52 dB and 60 dB, shown in (c), can be deduced to be caused by debonding or cracking of the embedded particulate fillers from the thermoset polymer matrix. Nevertheless, there appears to be a number of different mechanisms from those described previously which could also result in AE signals. AE signals along the entire body of the specimen could be evidence of that, see Fig. 4(e). This indicates that there must be other sources which emit AE signals during the test.

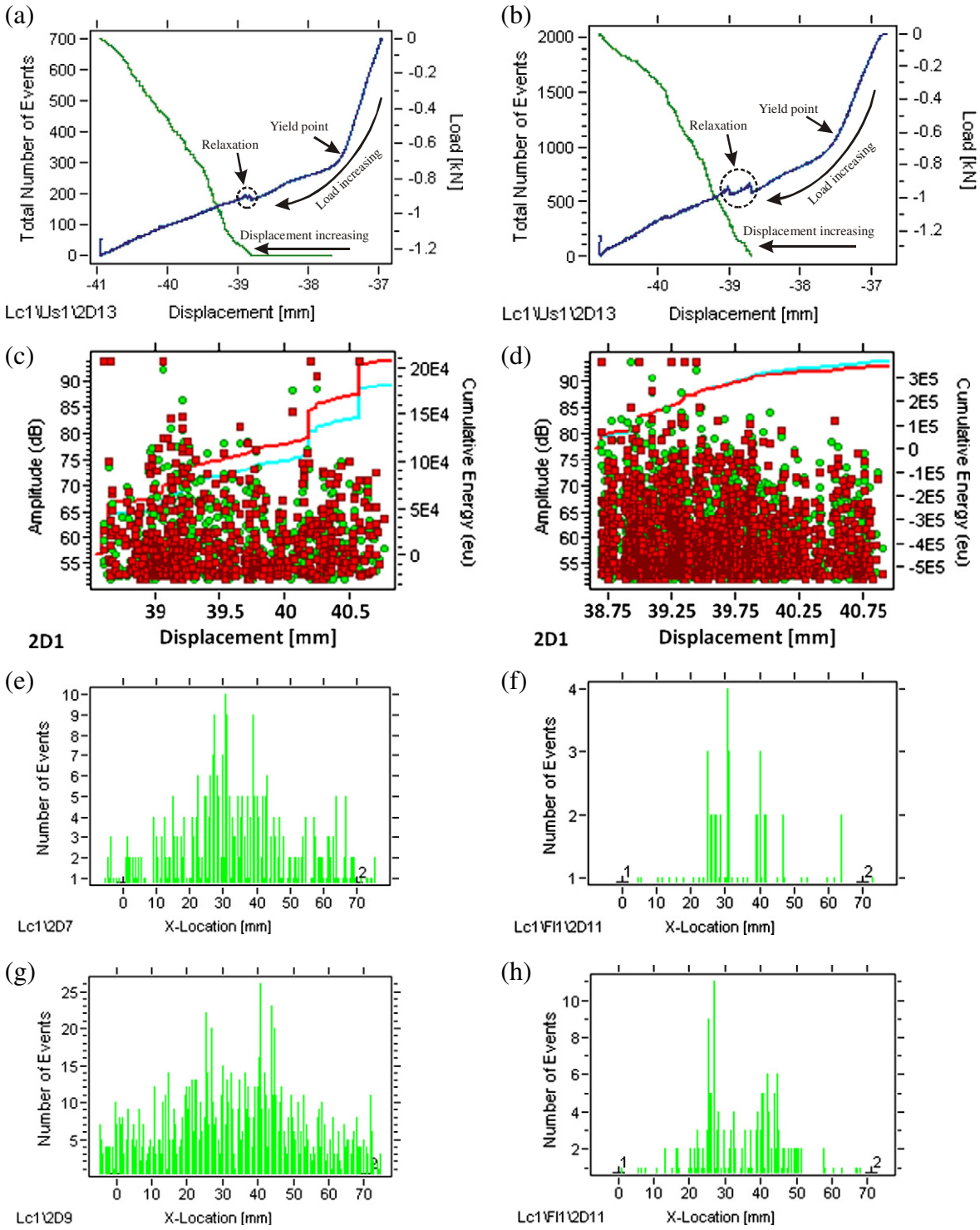

Fig. 4. Experimental results of four point bend tests with AE monitoring for the thermoset coatings T-15A and T-15B. (a) Load and total number of AE events as a function of displacement for sample T-15A. (b) Load and total number of AE events as a function of displacement for sample T-15B. (c) Amplitude distribution and cumulative energy of AE signals for sample T-15A in a four point bend test. (d) Amplitude distribution and cumulative energy of AE signals for sample T-15B in a four point bend test. (e) Position distribution of AE signals in a four point bend test for T-15A. (f) Position distribution of AE signals in a four point bend test for T-15A, with filtering condition 70 dB ≤ Amplitude ≤ 95 dB. (g) Position distribution of AE signals in a four point bend test for T-15B. (h) Position distribution of AE signals in a four point bend test for T-15B, with filtering condition 70 dB ≤ Amplitude ≤ 95 dB.

Possible sources could be the reflection of the longitudinal waves from the crack sidewall.

Similar results for the thick coating sample T-15B were obtained and are shown in Fig. 4(g) and (h). Since the only difference between the two specimens was their different coating thickness the mechanisms causing the AE signals for the two specimens are believed to be the same, thus a similar explanation on the mechanisms generating the AE signals on T-15A can be applied to T-15B. The limited number of high amplitude events, which occurred only during the first 2.5 mm deflection of the test sample, agreed with the fewer cracks observed on the surface of the T-15B coating. A greater number of AE signals with lower amplitudes close to the

macrocracks on the thick coating T-15B was observed and the cumulative energy measured was higher at the end of the test for T-15B than for T-15A. This correlates with the greater amount of delamination observed in the thick coating T-15B, as shown in Fig. 3. The greater cumulative energy measured is also caused by the larger number of embedded filler particles present in the thicker coating T-15B than in the thinner coating which debond or crack during the test. The different size of delamination between thick and thin coating samples was caused by the different shear stress along the boundary between coating and steel substrate. Since the closer to the neutral axis of the sample the higher is the shear stress, for the present test sample structure the boundary line of the thick coating is closer to the neutral axis of the sample than that of the thin coating, therefore a higher shear stress was applied to the boundary between the thicker coating and its steel substrate. Hence, under the same conditions of coating the sample with the thicker coating is more likely to suffer delamination.

Fig. 4(f) and (h) indicates that no high amplitude AE events caused by the initiation and propagation of cracks occurred at the position of the rollers in contact with the coating (16 and 56 mm); the total number of AE events at these locations compared with at other positions was not prominent when no filter conditions were applied as shown in Fig. 4(e) and (g), although the two AE sensors were attached close to the two outer ceramic rollers in contact with the coating surface, as shown in Fig. 2. This was consistent with the appearance of the two coating samples after testing shown in Fig. 3(a) and (b), i.e. no damage, in the form of cracks or severe plastic deformation, occurred on the two thermoset coatings at the contacting positions of the ceramic rollers. This again indicates that the direct contact between the ceramic rollers and the coatings surface in the experiment setup did not influence the AE experimental results or data analysis.

3. Conclusions

Two particulate filled thermoset coating samples T-15A and T-15B with different coating thicknesses have been investigated using the four point bend test with AE monitoring. The influence of the fillers and the thicknesses of the coatings on the overall mechanical properties of the test samples have been discussed. The relationship between the AE signals and the damage mechanisms of the coatings under the bend test has been correlated. The following main conclusions can be drawn from the analysis of the test results:

1. The development and propagation of cracks in the particulate filled polymeric coatings with low value of elastic modulus (<20 GPa) on the steel substrate can generate a noticeable load drop on the load – displacement curve when the whole test sample behaves plastically with a much smaller apparent modulus. A load drop is not expected when the sample behaves elastically when the Young's modulus of steel (207 GPa) dominates the stiffness of the whole sample.
2. When delamination between the coating and the steel substrate is not extensive further load applied to the polymeric coating samples will lead to more but smaller load drops associated with further cracks.
3. From the positions of the AE signals, the regions around the cracks can be located, although the precise positions are difficult to determine due to experimental set up error.
4. The amplitude of the AE signals obtained during the four point bend tests for the coating samples could be correlated with the phenomena occurring in the test. Therefore, damage mechanisms can be distinguished at a glance from the amplitude of the events.
5. Extensive delamination was found close to the macrocracks on the thicker coating sample and small delaminations were found on the thinner coating sample. The larger shear stresses present at the interface for the thicker coating might be responsible for this.

Acknowledgements

Authors acknowledge financial support from the School of Engineering Sciences, University of Southampton and B. P. Exploration, Sunbury-on-Thames, UK.

References

[1] J.T. Dickinson, A. Jahan-Latibari, L.C. Jensen, Journal of Materials Science 20 (1985) 229.
[2] R.J. Boness, S.L. McBride, M. Sobczyk, Tribology International (1990) 291.
[3] M. Schossig, A. Zankel, C. Bierogel, et al., Composites Science and Technology 71 (2011) 257.
[4] J.M. Miguel, J.M. Guilemany, Y.M. Xu, B.G. Mellor, Materials Science and Engineering A352 (2003) 55.
[5] C. Richard, G. Beranger, J. Lu, F. Flavenot, T. Gregoire, Surface Coating Technology 78 (1996) 284.
[6] C.K. Lee, J.J. Scholey, et al., Corrosion Engineering Science and Technology 43 (2008) 54.
[7] C. Scruby, Journal of Physics, E: Science Instrumentation 20 (1987) 946.
[8] L. Jacobs, Journal of Engineering Mechanics 117 (1991) 1878.
[9] M. Jerabek, Z. Major, et al., Polymer 51 (2010) 2040.
[10] A.R. Oskouei, M. Ahmadi, Journal of Composite Materials 44 (2010) 793.
[11] R. Kraus, W. Wilke, A. Zhuk, et al., Investigation of debonding processes in particle filled polymer materials by acoustic emission Part II Acoustic emission amplitude and energy release by debonding, Journal of Materials Science 32 (1997) 4405.
[12] Z.Y. Piao, B.S. Xu, H.D. Wang, et al., Applied Surface Science 257 (2011) 2581.
[13] D. Dalmas, S. Benmedakhene, C. Richard, A. Laksimi, Characterization of Cracking Within WC-Co Coated Materials by an Acoustic Emission Method During Four Points Bending Tests, Thermal Spray, Surface Engineering Via Applied Research, ASM International, 2000, p. 1335.
[14] R.V. Sagar, B.K.R. Prasad, Magazine of Concrete Research 61 (2009) 419.
[15] F.E. Silva, L.L. Goncalves, et al., Chaos Solitons & Fractals 26 (2005) 481.
[16] I.M. De Rosa, C. Santulli, F. Sarasini, Journal of Applied Polymer Science 119 (2011) 1366.
[17] S. Arul, L. Vijayaraghavan, S.K. Malhotra, Journal of Materials Processing Technology 185 (2007) 184.
[18] T. Czigány, Composites Science and Technology 66 (2006) 3210.
[19] M.G.R. Sause, F. Haider, S. Horn, Surface & Coatings Technology 204 (2009) 300.
[20] Y. Shinhara, K. Ohtani, T. Tokuda, et al., Modern Physics Letters B 22 (2008) 839.
[21] M.C. Horrillo, J.L. Fontecha, I. Sayago, Thin Solid Films 467 (2004) 234.
[22] M. Fregonese, L. Jaubert, Y. Cetre, Progress in Organic Coatings 59 (2007) 239.